

Direct Adversarial Training: An Adaptive Method to Penalize Lipschitz Continuity of the Discriminator

Ziqiang Li, Pengfei Xia, Rentuo Tao, Hongjing Niu, Bin Li *Member, IEEE*

Abstract—Generative Adversarial Networks (GANs) are the most popular image generation models that have achieved remarkable performance on various tasks. However, training instability is still one of the open problems for all GAN-based algorithms. In order to stabilize GANs training, some regularization and normalization techniques have been proposed to make the discriminator meet the Lipschitz continuity. In this paper, a new approach inspired by works on adversarial is proposed to stabilize the training process of GANs. It is found that sometimes the images generated by the generator play a role just like adversarial examples for discriminator during the training process, which might be a part of the reason for the unstable training of GANs. With this discovery, we propose a Direct Adversarial Training (DAT) method for the training process of GANs to improve its performance. We prove that the DAT method can minimize the Lipschitz constant of the discriminator adaptively. The advanced performance of the proposed method is verified on multiple baseline and SOTA networks, such as DCGAN, Spectral Normalization GAN, Self-supervised GAN, and Information Maximum GAN. Code will be available at <https://github.com/iceli1007/DAT-GAN>

Index Terms—Adversarial training, Generative adversarial networks, Lipschitz.

I. INTRODUCTION

Recently, Generative Adversarial Networks (GANs) [1] have been used in many generative tasks, such as image inpainting [2], [3], attribute editing [4], [5], and adversarial examples [6], [7]. GANs is a two-player zero-sum game, in which the discriminator measures the distance between generated and real distributions, while the generator tries to fool the discriminator by minimizing the distance between real and generated distributions. Specifically, the optimal discriminator of vanilla GAN [1] estimates the JS divergence, optimal discriminators of f -GAN [8] and WGAN [9] estimate the f divergence and Wasserstein divergence, respectively. Although various types of GANs have shown impressive performance in many tasks, the training of GANs remains quite unstable, and this instability remains difficult to understand theoretically.

There are many techniques proposed to stabilize GANs training, including works of loss functions [9], [10], regularization and normalization technologies [11], [12], training

algorithms [13], [14], and model architectures [15], [16]. Notably, Wasserstein GAN (WGAN) [9] is proposed to avoid the instability caused by mismatched generator and data distribution supports. The optimal discriminator of WGAN can be considered as estimating the Wasserstein distance of two distributions. To solve the Kantorovich duality problem [17] of the Wasserstein distance, the discriminator should meet the 1-Lipschitz continuity, which is the first time that Lipschitz continuity has been introduced into the design of GANs. Except for 1-Lipschitz continuity in WGANs, Lipschitz continuity is also important for generalizability and distributional consistency for all GANs [18]. Qi [18] proved that, for the discriminator with Lipschitz continuous, the generated distributions converge to the real distributions in GANs. In practice, gradient penalties [11] and spectral normalization [12] are used to implement the Lipschitz continuity.

Different from the above aspects, we mainly consider the adversarial examples of the discriminator. Vulnerable to adversarial examples [19] is a defect that often occurs in neural networks. Small perturbations added on input samples can incur error predictions like misclassification even for the most advanced deep neural networks. Empirically, the most effective strategy to defend against adversarial attacks is adversarial training [20], which uses adversarial examples to train the classifier improving the robustness of the models. Inspired by adversarial examples in deep neural networks, we argue that the instability of GANs' training has close relation with adversarial examples generated by the generator. For GANs, parameter update of the generator is affected by gradient of the discriminator. However, adversarial examples of the discriminator make non-informative adversarial noises into the gradient of the discriminator, which influences the stability of GANs training.

First, we do a confirmatory experiment that attacks the discriminator of DCGAN [21]. The results are illustrated in Fig.1. The success of the attack is defined as:

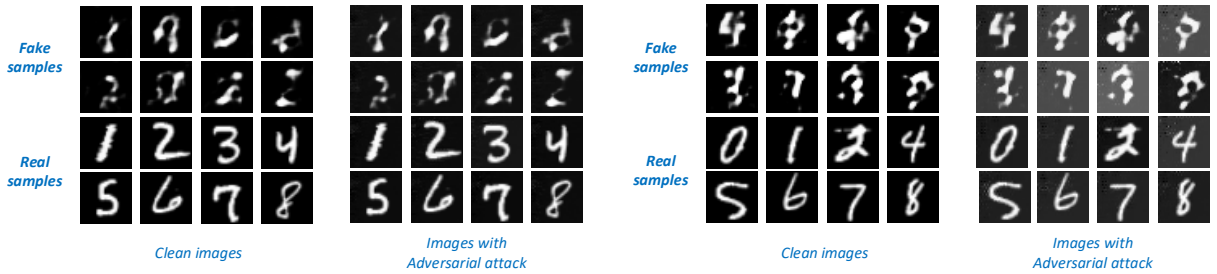
$$\begin{aligned} |D(\hat{x}_f) - D(x_r)| &\leq 0.02, \\ |D(\hat{x}_r) - D(x_f)| &\leq 0.02, \end{aligned} \quad (1)$$

where D represents the discriminator, x_f and x_r denote fake images generated by the non-convergent generator and real images sampled from train datasets, respectively. \hat{x}_f and \hat{x}_r are adversarial examples of generated images and real images, respectively. Fig.1 (a) illustrates that average iterations for successfully attacking a discriminator without adversarial training are 3.2 and 3.88, which indicates that vanilla GAN models can be easily attacked. Also, we can not distinguish between clean images and adversarial examples, intuitively.

This paper was submitted on May 5, 2021. This work was partially supported by National Natural Science Foundation of China under grant No.U19B2044, No.61836011.

Ziqiang Li, Pengfei Xia, Rentuo Tao, and Hongjing Niu are with the CAS Key Laboratory of Technology in Geo-spatial Information Processing and Application Systems, University of Science and Technology of China, Anhui, China. (E-mail: {iceli,xpengfei,rtmelon,sasori}@mail.ustc.edu.cn)

Bin Li (Corresponding author) is with the CAS Key Laboratory of Technology in Geo-spatial Information Processing and Application Systems, University of Science and Technology of China, Anhui, China. (E-mail: binli@ustc.edu.cn)



(a) adversarial attack without the adversarial training
 $(\bar{K}_{fake} = 3.2, \bar{K}_{real} = 3.88)$

(b) adversarial attack with the adversarial training
 $(\bar{K}_{fake} = 37.36, \bar{K}_{real} = 7.44)$

Fig. 1: Adversarial attack with the discriminator. (a) and (b) are the adversarial examples when DCGAN has no adversarial training and adversarial training on the MNIST dataset, respectively. The top two lines are the fake samples that are generated by generator without convergence. The bottom two lines are real samples from the MNIST dataset. \bar{K}_{fake} and \bar{K}_{real} are the average number of iterations when fake images and real images are successfully attacked, respectively

Since the model is assumed to have infinite capacity [1], without any prior, the generator has a high probability to generate adversarial examples that can mislead the discriminator. Moreover, we also provide proof of the existence of adversarial examples in the following chapters. To avoid the above-mentioned unstable threats, this paper proposes a method called Direct Adversarial Training (DAT) for GANs' training, which improves the robustness to hyperparameters and the quality of the generated images. More importantly, the proposed DAT can be considered as an **adaptive gradient penalty** method.

The main contributions can be summarized as follows:

- We prove that the generator may generate adversarial examples of the discriminator during the training of GANs and analyze the adversarial attack of the discriminator for the first time.
- We propose Direct Adversarial Training (DAT) for stabilizing the training process of GANs and prove that the DAT can **adaptively** minimize Lipschitz Continuity of the discriminator, which is different from the gradient penalty proposed by previous works.
- Without excessive cost, our method surprisingly improves the quality of the generated images on many basic and SOTA models.

II. BACKGROUND AND RELATED WORK

A. Generative Adversarial Networks

GANs is a two-player zero-sum game, where the generator $G(z)$ is a distribution mapping function that transforms low-dimensional latent distribution z into the target images distribution p_g . The generator is trained with another network $D(x)$, which evaluates the distance between generated distribution p_g and real distribution p_r . The generator and discriminator minimize and maximize the distribution distance respectively. This minimax game can be expressed as follows:

$$\min_{\phi} \max_{\theta} f(\phi, \theta) = \mathbb{E}_{x \sim p_r} [g_1(D_{\theta}(x))] + \mathbb{E}_{z \sim p_z} [g_2(D_{\theta}(G_{\phi}(z)))], \quad (2)$$

where ϕ and θ are parameters of the generator G and discriminator D , respectively. Specifically, vanilla GAN [1] can be described by $g_1(t) = g_2(-t) = -\log(1 + e^{-t})$, f -GAN [8] and WGAN [9] can be written as $g_1(t) = -e^{-t}$, $g_2(t) = 1 - t$ and $g_1(t) = g_2(-t) = t$, respectively.

B. Lipschitz Constant and WGAN

Lipschitz constant of the function $f : X \rightarrow Y$ is defined by:

$$\|f\|_L = \sup_{x, y \in X; x \neq y} \frac{\|f(x) - f(y)\|}{\|x - y\|}. \quad (3)$$

For a given constant $K \geq 0$ and any variables $x, y \in X$, the function f satisfies the K-Lipschitz continuity when and only when $\|f(x) - f(y)\| \leq K\|x - y\|$. Furthermore, Lipschitz constant of the neural network can be approximated by spectral norm of the weight matrix [22]:

$$\|W\|_2 = \max_{x \neq 0} \frac{\|Wx\|}{\|x\|}. \quad (4)$$

The Lipschitz constant can be used to express the Lipschitz continuity of the neural network. Lower Lipschitz constant means that the neural network is less sensitive to input perturbation and the bounded Lipschitz constant indicates that the network has better generalization [23], [24], [25].

For GANs, a lot of works are proposed to limit the Lipschitz constant of the discriminator, such as spectral normalization [12] and WGAN [9]. Spectral normalization normalizes the spectral norm of the discriminator, which limits its Lipschitz constant to 1. And the Lipschitz constant in WGAN is derived from Kantorovich duality [17], the Wasserstein distance corresponding to the optimal transportation can be represented as:

$$W(P_1, P_2) = \sup_{\|f\|_L=1} \mathbb{E}_{x \sim p_r} f(x) - \mathbb{E}_{x \sim p_g} f(x), \quad (5)$$

where $f : X \rightarrow \mathbb{R}$ is called the Kantorovich potential, which can be used as discriminator. To make the discriminator satisfy the Lipschitz continuity, WGAN [9] uses the weight clipping

which restricts the maximum value of each weight; WGAN-GP [11] uses the gradient penalty with the interpolation of real samples and generated samples: $\hat{x} = tx + (1 - t)y$ for $t \sim U[0, 1]$ and $x \sim P_r, y \sim P_g$ being a real and generated samples; WGAN-ALP [26] inspired by Virtual Adversarial Training (VAT) [27] restricts the 1-Lipschitz continuity at $\hat{x} = \{x, y\}$ with the direction of adversarial perturbation. Different from the above methods which restrict the 1-Lipschitz continuity [11], [26], [28], [29], WGAN-LP [30] restricts the k -Lipschitz continuity ($k \leq 1$), which is derived from the optimal transport with regularization. Also, Qi. [18] is motivated to have lower sample complexity by directly minimizing the Lipschitz constant rather than constraining it to 1, which can be described as 0-GP [31], [32], [33]. In summary [22], there are many methods for restricting the Lipschitz constant, some restrict the constant to 1, some restrict it to k ($k \leq 1$), and some minimize the Lipschitz constant.

C. Adversarial Examples and Adversarial Training

Adversarial example is a common problem in neural networks. Given a pre-trained model h , adversarial examples x' are defined by $x' = x + \delta$ with $h(x') \neq h(x)$ for untargeted attack or $h(x') = t$ for targeted attack, where x is a clean image and δ is an imperceptible tiny perturbation. There are many methods to generate adversarial examples, such as Fast Gradient Sign Method (FGSM) [20], Basic Iterative Methods (BIM) [34], and Projected Gradient Descent (PGD) [35]. FGSM uses the single gradient step to generate adversarial examples:

$$\begin{cases} x' = x + \epsilon \cdot \text{sign}(\nabla_x \mathcal{L}(x, y)) & \text{for untargeted} \\ x' = x - \epsilon \cdot \text{sign}(\nabla_x \mathcal{L}(x, t)) & \text{for targeted} \end{cases}, \quad (6)$$

where \mathcal{L} is the loss function. PGD is a multi-step method which creates adversarial examples by iterative:

$$\begin{cases} x^{k+1} = \text{clip}(x^k + \alpha \cdot \text{sign}(\nabla_x \mathcal{L}(x^k, y))) & \text{for untargeted} \\ x^{k+1} = \text{clip}(x^k - \alpha \cdot \text{sign}(\nabla_x \mathcal{L}(x^k, t))) & \text{for targeted} \end{cases}, \quad (7)$$

where **clip** is the clip function, α is the step size of gradient, $x^0 = x$, $x' = x^K$, and K is the number of iterations. Besides, some works [36], [37] use GANs to generate adversarial examples.

Adversarial training is a good and simple method to avoid adversarial examples, which improves the robustness of the neural networks by:

$$\min_{\theta} \mathbb{E}_{x, y \sim D} [\max_{\|\delta\|_p \leq \epsilon} \mathcal{L}_{\theta}(x + \delta, y)], \quad (8)$$

where $x, y \sim D$ are sampled from the joint distribution of data (image, label), θ is the parameters of the model. This min-max problem is similar to the GANs, the main difference is that the independent variable of the maximization problem in the adversarial training is image samples x , rather than the discriminator parameters.

D. The Adversarial Robustness with GANs Training

Recently, some works begin to analyze the relationship between GANs training and adversarial robustness. RobGAN [38] is the first work to introduce adversarial training in GANs training, which adds the adversarial training for the classifier in cGANs. This method does not directly analyze adversarial examples of the discriminator. Furthermore, Zhou et al [39] analyze the non-robust characteristics of the discriminator for the first time. They propose the consistent regularization between clean images and adversarial images in the training of GANs, which will let the discriminator not be fooled by adversarial examples. As we all know, adversarial training is a remarkable method to improve adversarial robustness. Concurrent with our work, several methods [40], [41] independently propose adversarial training for the training of GANs. We urge the readers to check out their work for more details. Compared with concurrent works mentioned above, our paper analyzes the possibility of the generator to generate adversarial examples and the relationship between Direct Adversarial Training and adaptive Lipschitz minimum. Moreover, our work contains richer experiment results and better performance.

III. CONDITION OF ADVERSARIAL ATTACKING BY GENERATOR

In this section, we will prove the existence of the adversarial examples of discriminator during the GANs' training. Intuitively, the goals of adversarial training and generators' training are contradictory, while the goals of generator training and adversarial perturbation are the same. Both generator and adversarial perturbation hope that the generated distribution is closer to the true distribution under the metric of the discriminator.

Lemma 1: Assuming δ is adversarial perturbation, ϕ^t and ϕ^{t+1} are the parameters for the t -th and $(t+1)$ -th update of the generator. Then the generator may generate adversarial examples of the discriminator

Proof 1:

- Suppose that the loss function between the true distribution and the generated distribution measured by the discriminator is \mathcal{L} , the generator is single-layered network which can be represented as $G_{\phi}(z) = f(\phi \cdot z)$. Having:

$$\begin{aligned} D_{\theta}(G(z; \phi^{t+1})) &= D_{\theta}(G(z; \phi^t + \Delta\phi)) \\ &= D_{\theta}(f(z \cdot (\phi^t + \Delta\phi))) \\ &= D_{\theta}(f(z \cdot \phi^t) + \nabla f \Delta\phi \cdot z) \\ &= D_{\theta}(G_{\phi}(z) + \nabla f \Delta\phi \cdot z) \end{aligned} \quad (9)$$

where $\Delta\phi = \phi^{t+1} - \phi^t$ is the updated value of the generator parameters, f is activation function. If using SGD, then $\Delta\phi = \frac{\partial \mathcal{L}}{\partial \phi}$. Also the adversarial perturbation $\delta = \frac{\partial \mathcal{L}}{\partial G_{\phi}(z)}$. For $\frac{\partial \mathcal{L}}{\partial \phi} = \frac{\partial \mathcal{L}}{\partial G_{\phi}(z)} \nabla f \cdot z$, having:

$$D_{\theta}(G(z; \phi^{t+1})) = D_{\theta}(G_{\phi}(z) + \delta \nabla^2 f \cdot z^2) \quad (10)$$

If $\nabla^2 f \cdot z^2 = 1$, then the generator will generate the adversarial examples of the discriminator.

- If the generator is two-layered, which can be represented as $G_\phi(z) = f_2(\phi_2 \cdot f_1(\phi_1 \cdot z))$. Having:

$$D_\theta(G(z; \phi^{t+1})) = D_\theta(G(z; \phi^t + \Delta\phi)) \quad (11)$$

$D_\theta(G(z; \phi_1^{t+1}))$ can be writed as:

$$\begin{aligned} D_\theta(G(z; \phi_1^{t+1})) &= D_\theta(G(z; \phi_1^t + \Delta\phi_1)) \\ &= D_\theta(f_2(\phi_2^t \cdot f_1(z \cdot (\phi_1^t + \Delta\phi_1)))) \\ &= D_\theta(G_\phi(z) + \nabla f_2 \nabla f_1 \Delta\phi_1 \cdot \phi_2^t \cdot z) \end{aligned} \quad (12)$$

Now, the adversarial perturbation $\delta = \frac{\partial \mathcal{L}}{\partial G_\phi(z)}$. For $\frac{\partial \mathcal{L}}{\partial \phi_1} = \frac{\partial \mathcal{L}}{\partial G_\phi(z)} \nabla f_2 \nabla f_1 \cdot \phi_2 \cdot z$, having:

$$D_\theta(G(z; \phi_1^{t+1})) = D_\theta(G_\phi(z) + \delta \nabla^2 f_2 \nabla^2 f_1 \cdot \phi_2^t \cdot z^2) \quad (13)$$

Similarly, $D_\theta(G(z; \phi_2^{t+1}))$ can be writed as:

$$\begin{aligned} D_\theta(G(z; \phi_2^{t+1})) &= D_\theta(G(z; \phi_2^t + \Delta\phi_2)) \\ &= D_\theta(f_2((\phi_2 + \Delta\phi_2) \cdot f_1(z \cdot \phi_1^t))) \\ &= D_\theta(G_\phi(z) + \nabla f_2 \Delta\phi_2 f_1(\phi_1^t \cdot z)) \end{aligned} \quad (14)$$

Now, the adversarial perturbation $\delta = \frac{\partial \mathcal{L}}{\partial G_\phi(z)}$. For $\frac{\partial \mathcal{L}}{\partial \phi_2} = \frac{\partial \mathcal{L}}{\partial G_\phi(z)} \nabla f_2 \cdot f_1(\phi_1 \cdot z)$, having:

$$D_\theta(G(z; \phi_2^{t+1})) = D_\theta(G_\phi(z) + \delta \nabla^2 f_2 \cdot f_1^2(\phi_1 \cdot z)) \quad (15)$$

If $\nabla^2 f_2 \nabla^2 f_1 \cdot \phi_2^t \cdot z^2 = 1$ and $\nabla^2 f_2 \cdot f_1^2(\phi_1 \cdot z) = 1$, then the generator will generate the adversarial examples of the discriminator.

- Similarly, the multi-layered generator $G_\phi(z) = f_3(\phi_3 \cdot f_2(\phi_2 \cdot f_1(\phi_1 \cdot z)))$, which will also generate adversarial examples of the discriminator. The proof is similar to the previous two points. \square

From **Lemma 1**, we can see that adversarial examples can be generated by generator, which confirms the validity of our previous assumptions. The proof is not strict. We just explore the possibility of this phenomenon.

IV. PROPOSED APPROACH

Unlike previous adversarial training for classifiers, the proposed DAT method targets the discriminator that is a distribution metric function. The adversarial examples on the discriminator are defined as Eq (1), the unintentional attack for discriminator can be regarded as a targeted attack that minimizes the distance (under the discriminator) between the adversarial examples of the generated images and the real images, the same is true for adversarial examples of the real images.

In the following contents, we firstly introduce an adversarial perturbation strategy according to various distribution metrics, based on which the DAT method is proposed. Moreover, we also analyze the correlation between the proposed method and gradient penalty.

A. Adversarial Perturbation of the Discriminator

Most of the adversarial training is about classifiers, the goal of the classifier is fixed. For untargeted attacks, the direction of adversarial perturbation is the solution of $\max \mathcal{L}(x, y)$; and for targeted attacks, the direction of adversarial perturbation is the solution of $\min \mathcal{L}(x, t)$, where \mathcal{L} is the loss function of the classifiers. But for the discriminator, the goal of the output is dynamic, such as vanilla GAN, the outputs of the real images and fake images are both 0.5 for the optimal discriminator, but which is not true at the beginning of training. So the target of the output changes dynamically with training. Based on this, we propose a new adversarial perturbation for the discriminator. Defining the optimization problems as follows:

$$\begin{aligned} \delta(x_r) &= \arg \min \left| g_1(D_\theta(x_r + \delta(x_r))) - \overline{g_1(D_\theta(x_r))} \right| \\ \delta(x_f) &= \arg \min \left| g_2(D_\theta(x_f + \delta(x_f))) - \overline{g_2(D_\theta(x_r))} \right| \end{aligned} \quad (16)$$

where x_r and x_f are real image and generated image, respectively. $\delta(x_r)$ and $\delta(x_f)$ are adversarial perturbation of the real image x_r and generated image x_f , respectively. $\overline{g_1(D_\theta(x_r))}$ and $\overline{g_2(D_\theta(x_f))}$ are the average of the discriminator output in batches for the real and generated images, respectively. For above optimization problems in Eq (16), we use the one-step PGD attack to achieve it:

$$\begin{aligned} \delta(x_r) &= -\epsilon \nabla_{x_r} \left(\left| g_1(D(x_r)) - \overline{g_1(D(x_f))} \right| \right) \\ \delta(x_f) &= -\epsilon \nabla_{x_f} \left(\left| g_2(D(x_f)) - \overline{g_2(D(x_r))} \right| \right) \end{aligned} \quad (17)$$

where ϵ is perturbation level¹ and the goal of the adversarial perturbation changes with the training of the discriminator.

B. Direct Adversarial Training

Motivated by adversarial examples leading to unstable training of GANs, we propose an adversarial training method DAT for GANs in Fig.2. According to the loss function of GANs in Eq (2), the loss of GANs with DAT can be formed as:

$$\begin{aligned} \min_{\phi} \max_{\theta} f'(\phi, \theta) &= f_a(\phi, \theta) = \\ &= \mathbb{E}_{x \sim p_r} [g_1(D_\theta(x + \delta(x_r)))] + \mathbb{E}_{z \sim p_z} [g_2(D_\theta(G_\phi(z) + \delta(x_f)))] \end{aligned} \quad (18)$$

According to the above formulas, the complete algorithm is demonstrated in **Algorithm 1**.

C. Direct Adversarial Training and Lipschitz Continuity

In this part, we analyze the relationship between DAT and gradient penalty. The result demonstrates that our method can adjust the Lipschitz constant adaptively. The instability of GANs training is mainly caused by the discriminator, and our adversarial training is only for the discriminator, so we do not consider the generator at present. For adversarial perturbation

¹Generally, we set $\epsilon = 1$, while more discussion of the ϵ will be given in section 6.1

Algorithm 1 Direct Adversarial Training

Input: The batch size m , the real image distribution $P_r(x)$, the random noise $z \sim N(0, 1)$, the maximum number of training steps K , the number of steps to apply to the discriminator N , the loss function g_1 and g_2 .

Output: a fine-tuned generator G and discriminator D

```

1: for  $k=1, 2, \dots, K$  do
2:   for  $n=1,2, \dots, N$  do
3:     Draw  $m$  real samples  $x_r = \{x_r^{(1)}, x_r^{(2)}, \dots, x_r^{(m)}\}$  from the real data distribution  $p_r$ .
4:     Draw  $m$  latent noise  $z = \{z^{(1)}, z^{(2)}, \dots, z^{(m)}\}$  from the latent distribution  $p_z$ .
5:      $x_f = \{x_f^{(1)}, x_f^{(2)}, \dots, x_f^{(m)}\} = G_\phi(\{z^{(1)}, z^{(2)}, \dots, z^{(m)}\})$ 
6:      $\delta_f^{(i)} = -\epsilon \nabla_{x_f^{(i)}} \left( \left| g_1(D(x_f^{(i)})) - \bar{g}_1(D(x_r)) \right| \right)$  for  $i \in 1, 2, \dots, m$ 
7:      $\delta_r^{(i)} = -\epsilon \nabla_{x_r^{(i)}} \left( \left| g_2(D(x_r^{(i)})) - \bar{g}_2(D(x_f)) \right| \right)$  for  $i \in 1, 2, \dots, m$ 
8:      $x_{f-adv}^{(1)}, x_{f-adv}^{(2)}, \dots, x_{f-adv}^{(m)} = \{x_f^{(1)} + \delta_f^{(1)}, x_f^{(2)} + \delta_f^{(2)}, \dots, x_f^{(m)} + \delta_f^{(m)}\}$ 
9:      $x_{r-adv}^{(1)}, x_{r-adv}^{(2)}, \dots, x_{r-adv}^{(m)} = \{x_r^{(1)} + \delta_r^{(1)}, x_r^{(2)} + \delta_r^{(2)}, \dots, x_r^{(m)} + \delta_r^{(m)}\}$ 
10:    Update the discriminator by ascending its stochastic gradient:
        
$$\nabla_\theta \left\{ \frac{1}{m} \sum_{i=1}^m [g_1(D_\theta(x_{r-adv}^{(i)})) + g_2(D_\theta(x_{f-adv}^{(i)}))] \right\}$$

11:   end for
12:   Draw  $m$  latent noise  $\{z^{(1)}, z^{(2)}, \dots, z^{(m)}\}$ .
13:   Update the generator by descending its stochastic gradient:
        
$$\nabla_\phi \left\{ \frac{-1}{m} \sum_{i=1}^m [g_1(D_\theta(x_r^{(i)})) + g_2(D_\theta(G_\phi(z^{(i)})))] \right\}$$


```

```

14: end for
15: return

```

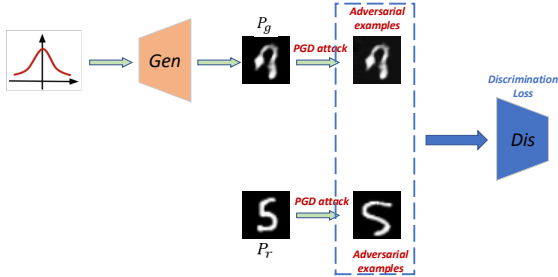


Fig. 2: Illustration of the proposed method. This is similar to the GANs training. The difference is that we add the one-step PGD attack for real and generated images, we hope that the discriminator not only can identify real or fake, but also be robust to adversarial examples

of real images $\delta(x_r) = -\epsilon \cdot \nabla_{x_r} \left(\left| g_1(D(x_r)) - \overline{g_1(D(x_f))} \right| \right)$, the loss function of the discriminator can be written as:

$$\begin{aligned} & \max_{\theta} \mathbb{E}_{x \sim p_r} \left[g_1(D_\theta(x + \delta(x))) \right] \\ & \approx \max_{\theta} \mathbb{E}_{x \sim p_r} \left[g_1(D_\theta(x)) + \nabla_x g_1(D_\theta(x)) \cdot \delta(x) \right]. \end{aligned} \quad (19)$$

For loss function of the Eq (19):

$$\begin{aligned} & g_1(D_\theta(x_r)) + \nabla_{x_r} g_1(D_\theta(x_r)) \cdot \delta(x_r) \\ & = g_1(D_\theta(x_r)) - \epsilon \nabla_{x_r} g_1(D_\theta(x_r)) \\ & \quad \cdot \nabla_{x_r} \left| g_1(D_\theta(x_r)) - \overline{g_1(D_\theta(x_f))} \right| \\ & = g_1(D_\theta(x_r)) - \epsilon g_1' \nabla_{x_r} D_\theta(x_r) \\ & \quad \cdot \nabla_{x_r} \left| g_1(D_\theta(x_r)) - \overline{g_1(D_\theta(x_f))} \right|. \end{aligned} \quad (20)$$

Because x_f is sampled from fake images, which is independent of x_r , when $g_1(D_\theta(x_r)) - \overline{g_1(D_\theta(x_f))} \geq 0$, it is true in most cases, the Eq (20) is $g_1(D_\theta(x_r)) - \epsilon g_1'^2 \nabla_{x_r}^2 D_\theta(x_r)$. In this case, $\max g_1(D_\theta(x_r)) - \epsilon g_1'^2 \nabla_{x_r}^2 D_\theta(x_r)$ is equivalent to adding gradient minimization to loss function, which can be seen as 0-GP. 0-GP can be used to limit the Lipschitz constant and stabilize the training of GANs. Also when $g_1(D_\theta(x_r)) - \overline{g_1(D_\theta(x_f))} < 0$, which means that the discriminator is trained incorrectly, the Eq (20) is $g_1(D_\theta(x_r)) + \epsilon g_1'^2 \nabla_{x_r}^2 D_\theta(x_r)$. In this case, $\max g_1(D_\theta(x_r)) + \epsilon g_1'^2 \nabla_{x_r}^2 D_\theta(x_r)$ means that we hope the discriminator will have a large change for perturbation, so as to jump out of the situation of wrong discrimination.

For adversarial perturbation of generated images $\delta(x_f) = -\epsilon \nabla_{x_f} \left(\left| g_2(D(x_f)) - \overline{g_2(D(x_r))} \right| \right)$, where $x_f = G_\phi(z)$. Update of the discriminator can be written as:

$$\begin{aligned} & \max_{\theta} \mathbb{E}_{x \sim p_f} \left[g_2(D_\theta(x + \delta(x))) \right] \\ & \approx \max_{\theta} \mathbb{E}_{x \sim p_f} \left[g_2(D_\theta(x)) + \nabla_x g_2(D_\theta(x)) \cdot \delta(x) \right]. \end{aligned} \quad (21)$$

We can get the loss function similar to the real images:

$$g_2(D_\theta(x_f)) - \epsilon g_2' \nabla_{x_f} D_\theta(x_f) \cdot \nabla_{x_f} \left| g_2(D_\theta(x_f)) - \overline{g_2(D_\theta(x_r))} \right|. \quad (22)$$

When $g_2(D_\theta(x_f)) \geq \overline{g_2(D_\theta(x_r))}$, the Eq (22) is $g_2(D_\theta(x_f)) - \epsilon g_2' \nabla_{x_f}^2 D_\theta(x_f)$. For generated images x_f , usually, $g_2(D_\theta(x_f))$ is greater than $g_2(D_\theta(x_r))$, in this case the adversarial training is equivalent to 0-GP; and $g_2(D_\theta(x_f)) < \overline{g_2(D_\theta(x_r))}$ indicates that the discriminator has an error and may get the local saddle point, so we maximize the gradient of the discriminator $\nabla_{x_f}^2 D_\theta(x_f)$, which can make the discriminator jump out of the error point as soon as possible.

From the above analyses, it can be seen that our proposed DAT can adaptively minimize the Lipschitz continuity, which is equivalent to 0-GP when the discriminator performance is better, and relax the limit on the Lipschitz constant when the discriminator performance is poor.

V. EXPERIMENTS

In this section, we implement the proposed DAT for DC-GAN, Spectral Normalization GAN (SNGAN) [12], Self-supervised GAN (SSGAN) [42], and Information Maximum GAN (InfoMAXGAN) [43]. Furthermore, we use three metrics to evaluate the performance of the methods: Fréchet Inception Distance (FID) [48], Kernel Inception Distance (KID) [49], and Inception Score (IS) [50]. In general, FID and KID measure the diversity between real and generated images, and IS only uses generated images to measure the quality. So we use train and test datasets to calculate FID and KID, respectively.

We test our method on the following datasets:

- The 2D synthetic dataset is created by this paper that contains two tiny sets: balanced mixture and imbalanced mixture. Both sets are sampled from a 2D mixture distribution of nine Gaussians, where the variance of the Gaussians distribution is 0.1, covariance is 0, and means are $\{-1, 0, 1\}$. The probability of each Gaussian distribution in the balanced mixture is equal, while the probabilities of Gaussian distribution in the imbalanced mixture are 0.15, 0.05, 0.8 from left to right. The visualizations are illustrated in (a) and (h) of Figure 3, respectively.
- The CIFAR-10 dataset comprises 50K train images and 10K test images with a spatial resolution of 32×32 pixels and are divided equally into 10 classes, with 6,000 images per class. Thus we train GAN models and compute Train FID and Train KID on the train dataset with 50K images. Certainly, Test FID and Test KID are calculated on the test dataset with 10K images.
- The CIFAR-100 dataset is similar to the CIFAR-10 dataset that comprises 50K train images and 10K test images and are divided equally into 100 classes. Thus we train GAN models and compute Train FID and Train KID on the train dataset with 50K images. Certainly, Test FID and Test KID are calculated on the test dataset with 10K images.
- The STL-10 dataset contains 100K unlabeled images and 8K test images at 96×96 resolution. All images are

resized to 48×48 pixels. Thus we train GAN models on the whole unlabeled dataset and compute Train FID Train KID on the unlabeled dataset with random 50K images. Certainly, Test FID and Test KID are calculated on the test dataset with 8K images.

- The Tiny ImageNet dataset contains 200 image classes with 100K images for training and 10K images for testing. All images are of size 64×64 . Similarly, we train GAN models on the whole train dataset and compute Train FID and Train KID on the train dataset with 50K random images. Certainly, Test FID and Test KID are calculated on the test dataset with 10K images.
- The LSUN Bedroom dataset has approximately 3M images. We took out 10K of them as a test set which is used to calculate the Test FID and Test KID and train the models on the rest images. Certainly, we compute Train FID and Train KID on the training dataset with 50K random images.

A. Experiments on DCGAN

In this section, we use DCGAN to experiment on two datasets (the 2D synthetic dataset and The CIFAR-10 dataset) to show the advancement of our method. The first experiment demonstrates that our proposed DAT can accelerate the training of GANs and avoid mode collapse and the second experiment indicates that the proposed DAT is more robust to hyperparameters.

We use a four layers of fully-connected MLP with 64 hidden units per layer to model the generator and discriminator on the 2D synthetic dataset. The Fig.3 illustrates the qualitative results of different iterations. The first line is visualization results on a **balanced** mixture of nine Gaussians. DAT can speed up the generation. When iterating 2k times, the generated distribution with adversarial training is closer to the true distribution. Even after training 10k times, the GANs without adversarial training can not fit the real distribution well. Also, we evaluate the method on an **imbalanced** mixture of nine Gaussians in the second line. The results illustrate that standard DCGAN will lose some small probability distribution, resulting in mode collapse, and this phenomenon will be significantly improved after adding DAT.

Furthermore, we use DCGAN² to do some comparative experiments on the CIFAR-10 dataset [44]. As shown in Figure 4, under different hyperparameters, the proposed DAT improves the performance of the GANs. Especially when $lr=0.002$, $b1=0.5$, the standard DCGAN can not be trained due to the gradient vanishing, while DAT-GAN alleviates this situation eminently. The results indicate that our DAT method reduces the sensitivity to hyperparameters during the training of GANs.

² In this part, we do confirmatory experiments using DCGAN with the simple architecture. The dimension of the latent vector is set to 100. Generator and discriminator are all implemented by 4 convolution layers and BN layers. At the last, we use the Adam optimizer with the most popular hyperparameters.

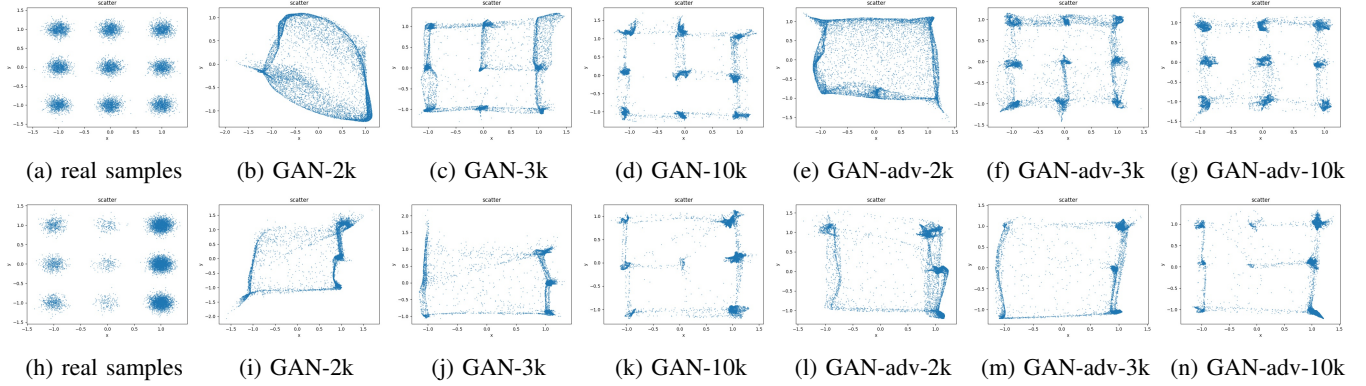


Fig. 3: Qualitative results of nine 2D-Gaussian synthetic data. The first line is a **balanced** Gaussian mixture distribution, and the second line is an **imbalanced** Gaussian mixture distribution. **First line:** (a): the real samples from a mixture of nine Gaussians. Where variance is 0.1 and means are $\{-1, 0, 1\}$; (b), (c) and (d): the results of iterating 2k times, 3k times, and 10k times in DCGAN; (e), (f) and (g): the results of iterating 2k times, 3k times, and 10k times in DCGAN with DAT. **Second line:** (h): the real samples from an imbalanced mixture of nine Gaussians. The probability of mixing Gaussian from left to right is 0.15, 0.05, 0.8. The other parts are the same as the first line

TABLE I: Training parameters on SOTA methods

Dataset	Resolution	Batch Size	Learning Rate	β_1	β_2	Decay Policy	n_{dis}	n_{iter}
CIFAR-10	32 x 32	64	2e-4	0.0	0.9	Linear	5	100K
CIFAR-100	32 x 32	64	2e-4	0.0	0.9	Linear	5	100K
STL-10	48 x 48	64	2e-4	0.0	0.9	Linear	5	100K
Tiny-ImageNet	64 x 64	64	2e-4	0.0	0.9	None	5	100K
LSUN-Bedroom	64 x 64	64	2e-4	0.0	0.9	Linear	5	100K

TABLE II: FID, KID, and IS scores of SOTA models across different datasets. FID and KID: lower is better. IS: higher is better.

Metric	Dataset	Evaluation set	Models					
			SNGAN	SNGAN-DAT	SSGAN	SSGAN-DAT	InfoMaxGAN	InfoMaxGAN-DAT
FID	LSUN-Bedroom	Train	27.26	24.10	23.54	20.43	35.69	34.21
		Test	86.10	83.50	85.10	82.20	87.14	86.17
	Tiny-ImageNet	Train	47.14	43.40	40.83	38.98	41.81	38.83
		Test	52.29	48.72	45.79	44.63	47.26	43.97
	STL-10	Train	42.62	41.05	39.84	35.64	42.39	40.77
		Test	62.03	60.41	56.56	52.71	61.93	59.07
	CIFAR-100	Train	23.70	21.09	22.43	19.86	21.36	20.46
		Test	28.48	26.49	27.61	24.67	26.36	25.28
CIFAR-10	Train	19.75	17.93	16.75	15.34	17.71	17.69	
	Test	24.19	22.46	21.23	19.45	22.03	21.88	
KID	LSUN-Bedroom	Train	0.0313	0.0286	0.0267	0.0246	0.0373	0.0369
		Test	0.0324	0.0296	0.0298	0.0275	0.0388	0.0375
	Tiny-ImageNet	Train	0.0411	0.0391	0.0355	0.0337	0.0371	0.0323
		Test	0.0415	0.0393	0.0371	0.0341	0.0372	0.0332
	STL-10	Train	0.0391	0.0380	0.0388	0.0336	0.0418	0.0384
		Test	0.0445	0.0428	0.0403	0.0352	0.0443	0.0404
	CIFAR-100	Train	0.0158	0.0160	0.0155	0.0147	0.0152	0.0140
		Test	0.0164	0.0161	0.0160	0.0148	0.0153	0.0142
	CIFAR-10	Train	0.0149	0.0133	0.0125	0.0116	0.0134	0.0128
		Test	0.0150	0.0142	0.0128	0.0118	0.0139	0.0141
	IS	LSUN-Bedroom	None	-	-	-	-	-
		Tiny-ImageNet	None	8.17	8.44	8.63	8.95	8.80
STL-10		None	8.34	8.45	8.59	8.72	8.28	8.57
CIFAR-100		None	7.66	7.82	7.74	8.09	8.02	8.06
CIFAR-10		None	7.84	7.97	8.13	8.25	8.01	8.07

TABLE III: Train FID scores on the CIFAR-10 dataset for various GAN losses and regularization methods.

loss	regularization								
	None	GP[11]	LP[30]	0-GP	AR[39]	RFM[39]	ASGAN[41]	DAT(ours)	DATT(DAT+T)
GAN[1]	30.20	27.80	27.25	29.76	29.37	27.89	27.24	26.98	26.77
LSGAN[53]	25.20	24.40	25.38	28.67	26.49	26.05	26.46	24.38	24.35
WGAN[9]	29.43	26.03	26.90	43.06	27.26	26.83	25.98	25.67	25.66

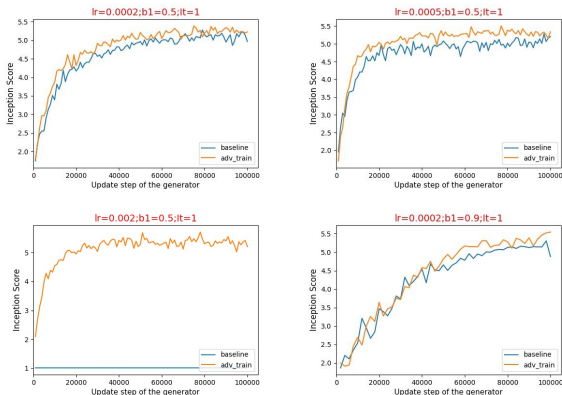


Fig. 4: The results of the DCGAN with different parameters in CIFAR-10. Where 'lr' is learning rate, 'b1' is the parameter of the Adam optimizer, and 't' is the ratio of the update times of the discriminator to the generator.

B. Evaluation on SOTA methods in different datasets

In this section, we use DAT on some SOTA methods, such as SNGAN, SSGAN and InfoMAXGAN. The architectures used for all models are equivalent to SNGAN. They can be available on Github³. We evaluate our method on five different datasets at multiple resolutions: CIFAR-10 (32×32) [44], CIFAR-100 (32 × 32) [44], STL-10 (48×48) [45], Tiny-ImageNet (64×64) [46], LSUN-Bedroom (64 × 64) [47]. All training parameters are selected with the best results on baseline networks. The details can be found in Table I, where the Adam parameters are Learning Rate (LR=2e-4), $\beta_1=0$ and $\beta_2=0.9$; n_{dis} is number of discriminator steps per generator step; n_{iter} is the trained times of the generator. Besides, we use the hinge loss to train all the models. Also, we use three metrics to evaluate the generated images quality: Fréchet Inception Distance (FID) [48], Kernel Inception Distance (KID) [49], and Inception Score (IS) [50]. The results are illustrated on Table II.

As seen in Table II, DAT improves FID, KID, and IS consistently and significantly across many datasets with three popular models. This suggests our approach is versatile and can generalize across multiple data domains. In particular, the usage of DAT greatly improved the FID of SSGAN on STL-10 dataset. Due to the large difference between the LSUN-Bedroom distribution and the ImageNet distribution, IS do not seem meaningful for it. So we do not show IS on LSUN-Bedroom dataset. Of course, there are some datasets where

SSGAN with DAT has the best performance, and in some datasets, InfoMaxGAN with DAT has the best performance. Furthermore, there has a gap between Train FID and Test FID, as [51], [52] said, GAN also exists overfitting. This may be the direction of our future work.

Furthermore, we also provide image samples randomly generated for all datasets in Appendix A.

C. The FID Results on CIFAR-10 Dataset with Other Regularization Method

From section 4.3, the proposed DAT can be considered as an adaptive gradient minimum (0-GP) method. To demonstrate the advancements of our method, we compare it with other regularization methods, such as GP, LP, 0-GP, AR, RFM, and ASGAN, on the CIFAR-10 dataset. To make the conclusion more general, we conduct comparative experiments on three loss functions of GANs (GAN [1], LSGAN [53], WGAN [9]). The baseline architecture and code use the implementation of AR and RFM, which can be available on Github⁴. From which, the dimensions of the latent vector is 128, the batch size is 64, and the Adam optimizer is set to $lr = 0.0001$, $\beta_1 = 0.5$, $\beta_2 = 0.999$.

We have implemented LP, 0-GP, ASGAN, DAT, and DATT based on the baseline code. LP is a relaxation constraint of GP, and it limits the gradient of the discriminator to k ($k \leq 1$). 0-GP minimizes the gradient of the discriminator, which is similar to the DAT with adaptive gradient minimization. AR and RFM propose the consistent regularization between clean images and adversarial images in the training of GANs, which will let the discriminator not be fooled by adversarial examples. ASGAN is another method using adversarial training for discriminator. However, like using adversarial training in classification tasks, the adversarial examples in ASGAN are generated by $\hat{x} = x - \epsilon \text{sign} \nabla_x (V_m(\theta, \phi, x, z))$, which is similar to the untargeted FGSM in Eq 6. $V_m(\theta, \phi, x, z)$ is the loss function of the discriminator. Here, we use the best-performing hyperparameter in [41], to be more specific, using FGSM $\epsilon = \frac{1}{255}$. DAT represents training the GANs as shown in Algorithm 1, while DATT represents training the network with adversarial examples and normal examples together. The Train FID results are illustrated in Table III, which confirm the advancements of our method. More specifically, we compare the generation results of 0-GP and DAT under the WGAN Loss, as shown in Figure 5. We find that the generation results on 0-GP with WGAN loss are very poor, which may be caused by the strict limit of minimizing the gradient penalty. DAT will

³https://github.com/kwotsin/mimicry

⁴https://github.com/bradyz/robust-discriminator-pytorch



Fig. 5: Randomly sampled images with 0-GP (left) and DAT (right) under the WGAN loss

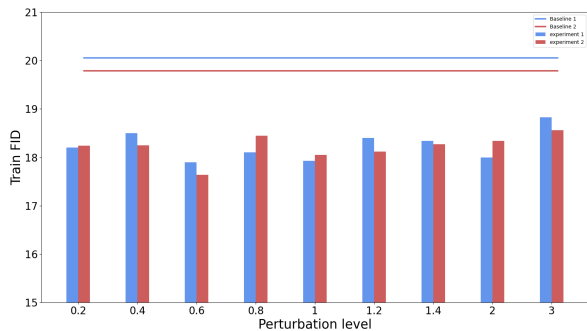


Fig. 6: Train FID scores in different ϵ settings of two independent runs (Lower is better)

adaptively minimize the gradient, which relieves the above limitation to improve the quality of the generation.

VI. EXPLORATORY AND ABLATION STUDIES

A. Evaluation with different perturbation levels

Perturbation level (ϵ in Eq (17)) is important for adversarial training. In this section, we evaluate the performance of the DAT on the CIFAR-10 dataset to investigate the effect of the different ϵ settings. Specifically, we perform unconditional image generation with SNGAN architecture in different settings of perturbation level. We select several typical values for experiments such as $\{0.2, 0.4, 0.6, 0.8, 1, 1.2, 1.4, 2, 3\}$. All experiments are conducted two times independently to reduce the effect of randomness.

As shown in Figure 6, the performance of the DAT is robust for the setting of ϵ . And the optimal setting of ϵ is around 1. From the perspective of perturbation, the tiny perturbation level improves the original model marginally. In this case, the effect of adversarial training is limited. On the contrary, the strong perturbation level affects the distribution of images, which reduces performance compared to the optimal parameter settings. Similarly, from the perspective of gradient penalty, a tiny penalty relaxes the restriction on the discriminator Lipschitz continuity, while a strong penalty leads to the tight restriction of the discriminator Lipschitz continuity. Both of them affect the performance of GANs.

B. Evaluation with different perturbation numbers

As acknowledged, in addition to the one-step adversarial perturbation mentioned in Section 4, adversarial training can be implemented by multi-step methods. Generally, these methods can be used to generate adversarial samples in DAT and are expected to achieve more appealing improvement. In this section, we experiment DAT method with different number of adversarial perturbations on the CIFAR-10 dataset, where the base architecture is SNGAN and the perturbation level ϵ is set to 0.6 and 1. We select several typical values for experiments such as $\{1, 2, 3, 4, 5\}$. All experiments are conducted two times independently to reduce the effect of randomness.

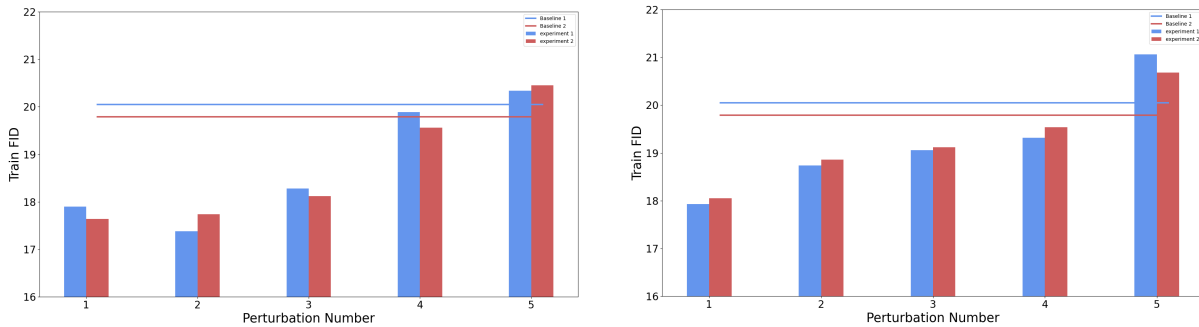
As shown in Figure 7, the left part illustrates the Train FID with $\epsilon = 0.6$ and the right part illustrates the Train FID with $\epsilon = 1$. DAT with multiple perturbation numbers achieves more significant improvement when the perturbation level is set to 0.6. However, the performance of GAN decreases with the number of perturbations when the perturbation level is set to 1. The results also demonstrate that neither too large nor too small adversarial perturbations are effective in improving the performance of GANs.

C. Evaluation with different perturbation positions

Different perturbation positions have different effects in adversarial training. In this section, we experiment the DAT with different positions of adversarial perturbation on the CIFAR-10 dataset, where the base architecture is SNGAN, the perturbation level is set to 1, and the perturbation number is set to 1. Figure 8 illustrates the overview of the DAT for updating discriminator and generator during GANs training, where (i), (ii), (iii) are different perturbation positions for DAT. The experimental results are shown in Table IV. From the results, the usage of the DAT on fake images ("Generator only" and "All" methods) destroys the training of GANs, which is caused by the gradient vanishing. Furthermore, using DAT only for fake images ("Fake only" method) or real images ("Real only" method) does not significantly improve the performance of GANs training. The best performance is as described in Algorithm 1, using DAT for real and fake images during discriminator training.

VII. CONCLUSIONS

Motivated by adversarial examples in neural networks, in this paper, we argue that the instability of GANs training has close relation with adversarial examples of the discriminator. Considerable adversarial noise of the discriminator misleads the update of the generator. With this discovery, we propose the Direct Adversarial Training (DAT) method to avoid the adversarial examples during discriminator training. Furthermore, the proposed DAT method can adaptively adjust the Lipschitz constants, which is superior to some fixed gradient penalty methods, such as GP, LP, and 0-GP. The validation on image generation on 2D synthetic, CIFAR-10, CIFAR-100, STL-10, Tiny ImageNet, and LSUN Bedroom datasets with varied network architectures demonstrates that DAT can significantly improve the performance and alleviating mode collapse. Besides, some ablation studies comparing the effect



(a) Train FID scores in different perturbation numbers of two independent runs ($\epsilon = 0.6$) (b) Train FID scores in different perturbation numbers of two independent runs ($\epsilon = 1$)

Fig. 7: Train FID scores in different perturbation numbers of two independent runs (Lower is better)

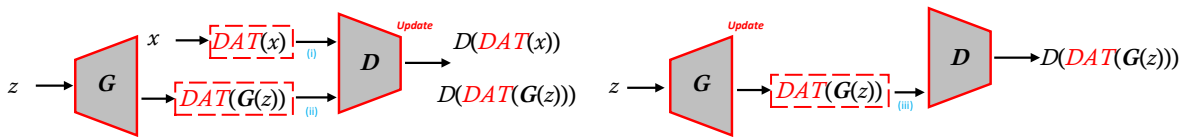


Fig. 8: Overview of the DAT for updating discriminator (left) and generator(right).

TABLE IV: The result with using DAT in different perturbation position for training the GANs on CIFAR-10 dataset. "Generator only" applies DAT to G (iii) (see Figure 8); "Real only" applies DAT to real (i); "Fake only" applies DAT to fake (ii); "Discriminator only" applies DAT to both real (i) and fake (ii), but not G (iii); "All" applies DAT to real (i), fake (ii), and G (iii). "Discriminator only" is described in section 4 and is used in other sections. We select the best FID score for each method during the training.

Method	Where <i>DAT</i> ?			Results				
	(i)	(ii)	(iii)	IS	Train_FID	Test_FID	Train_KID	Test_KID
SNGAN(Baseline)				7.84	19.75	24.19	0.0149	0.0150
SNGAN-DAT (Generator only)			✓	1.59	309	310.5	0.3836	0.3822
SNGAN-DAT (Real only)	✓			7.86	19.48	23.73	0.0147	0.0149
SNGAN-DAT (Fake only)		✓		7.84	19.64	24.1	0.015	0.0155
SNGAN-DAT (Discriminator only)	✓	✓		7.97	17.93	22.46	0.0133	0.0142
SNGAN-DAT (All)	✓	✓	✓	1.62	292	294	0.3603	0.3605

of different perturbation levels, numbers, and positions indicate that more complex adversarial manipulation methods can obtain further improvement.

ACKNOWLEDGMENT

The work is partially supported by the National Natural Science Foundation of China under grand No.U19B2044, No.61836011.

REFERENCES

- [1] I. Goodfellow, J. Pouget-Abadie, M. Mirza, B. Xu, D. Warde-Farley, S. Ozair, A. Courville, and Y. Bengio, "Generative adversarial nets," in *Advances in Neural Information Processing Systems*, 2014, pp. 2672–2680.
- [2] J. Yu, Z. Lin, J. Yang, X. Shen, X. Lu, and T. S. Huang, "Generative image inpainting with contextual attention," in *Proceedings of the IEEE Conference on Computer Vision and Pattern Recognition*, 2018, pp. 5505–5514.
- [3] R. A. Yeh, C. Chen, T. Yian Lim, A. G. Schwing, M. Hasegawa-Johnson, and M. N. Do, "Semantic image inpainting with deep generative models," in *Proceedings of the IEEE Conference on Computer Vision and Pattern Recognition*, 2017, pp. 5485–5493.
- [4] R. Tao, Z. Li, R. Tao, and B. Li, "Resattr-gan: Unpaired deep residual attributes learning for multi-domain face image translation," *IEEE Access*, vol. 7, pp. 132 594–132 608, 2019.
- [5] Y. Shen, J. Gu, X. Tang, and B. Zhou, "Interpreting the latent space of gans for semantic face editing," in *Proceedings of the IEEE Conference on Computer Vision and Pattern Recognition*, 2020, pp. 9243–9252.
- [6] C. Xiao, B. Li, J.-Y. Zhu, W. He, M. Liu, and D. Song, "Generating adversarial examples with adversarial networks," *arXiv preprint arXiv:1801.02610*, 2018.
- [7] Y. Song, R. Shu, N. Kushman, and S. Ermon, "Constructing unrestricted adversarial examples with generative models," in *Advances in Neural Information Processing Systems*, 2018, pp. 8312–8323.
- [8] S. Nowozin, B. Cseke, and R. Tomioka, "f-gan: Training generative neural samplers using variational divergence minimization," in *Advances in Neural Information Processing Systems*, 2016, pp. 271–279.
- [9] M. Arjovsky, S. Chintala, and L. Bottou, "Wasserstein gan," *arXiv preprint arXiv:1701.07875*, 2017.
- [10] A. Brock, J. Donahue, and K. Simonyan, "Large scale gan training for high fidelity natural image synthesis," 2019.
- [11] I. Gulrajani, F. Ahmed, M. Arjovsky, V. Dumoulin, and A. C. Courville, "Improved training of wasserstein gans," in *Advances in Neural Information Processing Systems*, 2017, pp. 5767–5777.
- [12] T. Miyato, T. Kataoka, M. Koyama, and Y. Yoshida, "Spectral normalization for generative adversarial networks," *arXiv preprint arXiv:1802.05957*, 2018.

- [13] M. Heusel, H. Ramsauer, T. Unterthiner, B. Nessler, and S. Hochreiter, “Gans trained by a two time-scale update rule converge to a local nash equilibrium,” 2018.
- [14] Y. Yaz, C.-S. Foo, S. Winkler, K.-H. Yap, G. Piliouras, V. Chandrasekhar *et al.*, “The unusual effectiveness of averaging in gan training,” in *International Conference on Learning Representations*, 2018.
- [15] T. Karras, T. Aila, S. Laine, and J. Lehtinen, “Progressive growing of gans for improved quality, stability, and variation,” *arXiv preprint arXiv:1710.10196*, 2017.
- [16] T. Karras, S. Laine, and T. Aila, “A style-based generator architecture for generative adversarial networks,” in *Proceedings of the IEEE/CVF Conference on Computer Vision and Pattern Recognition*, 2019, pp. 4401–4410.
- [17] L. V. Kantorovich, “On a problem of monge,” *J. Math. Sci.(NY)*, vol. 133, p. 1383, 2006.
- [18] G.-J. Qi, “Loss-sensitive generative adversarial networks on lipschitz densities,” *International Journal of Computer Vision*, vol. 128, no. 5, pp. 1118–1140, 2020.
- [19] C. Szegedy, W. Zaremba, I. Sutskever, J. Bruna, D. Erhan, I. Goodfellow, and R. Fergus, “Intriguing properties of neural networks,” *arXiv preprint arXiv:1312.6199*, 2013.
- [20] I. J. Goodfellow, J. Shlens, and C. Szegedy, “Explaining and harnessing adversarial examples,” *arXiv preprint arXiv:1412.6572*, 2014.
- [21] A. Radford, L. Metz, and S. Chintala, “Unsupervised representation learning with deep convolutional generative adversarial networks,” *arXiv preprint arXiv:1511.06434*, 2015.
- [22] Z. Li, R. Tao, and B. Li, “Regularization and normalization for generative adversarial networks: A review,” *arXiv preprint arXiv:2008.08930*, 2020.
- [23] Y. Yoshida and T. Miyato, “Spectral norm regularization for improving the generalizability of deep learning,” *arXiv preprint arXiv:1705.10941*, 2017.
- [24] A. M. Oberman and J. Calder, “Lipschitz regularized deep neural networks converge and generalize,” *arXiv preprint arXiv:1808.09540*, 2018.
- [25] N. Couellan, “The coupling effect of lipschitz regularization in deep neural networks,” *arXiv preprint arXiv:1904.06253*, 2019.
- [26] D. Terjék, “Adversarial lipschitz regularization,” in *International Conference on Learning Representations*, 2019.
- [27] T. Miyato, S.-i. Maeda, M. Koyama, and S. Ishii, “Virtual adversarial training: a regularization method for supervised and semi-supervised learning,” *IEEE Transactions on Pattern Analysis and Machine Intelligence*, vol. 41, no. 8, pp. 1979–1993, 2018.
- [28] N. Kodali, J. Abernethy, J. Hays, and Z. Kira, “On convergence and stability of gans,” *arXiv preprint arXiv:1705.07215*, 2017.
- [29] Z. Zhou, J. Shen, Y. Song, W. Zhang, and Y. Yu, “Towards efficient and unbiased implementation of lipschitz continuity in gans,” *arXiv preprint arXiv:1904.01184*, 2019.
- [30] H. Petzka, A. Fischer, and D. Lukovnicov, “On the regularization of wasserstein gans,” *arXiv preprint arXiv:1709.08894*, 2017.
- [31] Z. Zhou, J. Liang, Y. Song, L. Yu, H. Wang, W. Zhang, Y. Yu, and Z. Zhang, “Lipschitz generative adversarial nets,” *arXiv preprint arXiv:1902.05687*, 2019.
- [32] L. Mescheder, A. Geiger, and S. Nowozin, “Which training methods for gans do actually converge?” *arXiv preprint arXiv:1801.04406*, 2018.
- [33] H. Thanh-Tung, T. Tran, and S. Venkatesh, “Improving generalization and stability of generative adversarial networks,” *arXiv preprint arXiv:1902.03984*, 2019.
- [34] A. Kurakin, I. Goodfellow, and S. Bengio, “Adversarial machine learning at scale,” *arXiv preprint arXiv:1611.01236*, 2016.
- [35] A. Madry, A. Makelov, L. Schmidt, D. Tsipras, and A. Vladu, “Towards deep learning models resistant to adversarial attacks,” *arXiv preprint arXiv:1706.06083*, 2017.
- [36] W. Hu and Y. Tan, “Generating adversarial malware examples for black-box attacks based on gan,” *arXiv preprint arXiv:1702.05983*, 2017.
- [37] P. Samangouei, M. Kabkab, and R. Chellappa, “Defense-gan: Protecting classifiers against adversarial attacks using generative models,” *arXiv preprint arXiv:1805.06605*, 2018.
- [38] X. Liu and C.-J. Hsieh, “Rob-gan: Generator, discriminator, and adversarial attacker,” in *Proceedings of the IEEE Conference on Computer Vision and Pattern Recognition*, 2019, pp. 11 234–11 243.
- [39] B. Zhou and P. Krähenbühl, “Don’t let your discriminator be fooled,” in *International Conference on Learning Representations*, 2018.
- [40] S. Zhang, Z. Qian, K. Huang, J. Xiao, and Y. He, “Robust generative adversarial network,” *arXiv preprint arXiv:2004.13344*, 2020.
- [41] F. Liu, M. Xu, G. Li, J. Pei, L. Shi, and R. Zhao, “Adversarial symmetric gans: Bridging adversarial samples and adversarial networks,” *Neural Networks*, 2020.
- [42] T. Chen, X. Zhai, M. Ritter, M. Lucic, and N. Houlsby, “Self-supervised gans via auxiliary rotation loss,” in *Proceedings of the IEEE Conference on Computer Vision and Pattern Recognition*, 2019, pp. 12 154–12 163.
- [43] K. S. Lee, N.-T. Tran, and N.-M. Cheung, “Infomax-gan: Improved adversarial image generation via information maximization and contrastive learning,” *arXiv preprint arXiv:2007.04589*, 2020.
- [44] A. Krizhevsky, G. Hinton *et al.*, “Learning multiple layers of features from tiny images,” 2009.
- [45] A. Coates, A. Ng, and H. Lee, “An analysis of single-layer networks in unsupervised feature learning,” in *Proceedings of the International Conference on Artificial Intelligence and Statistics*, 2011, pp. 215–223.
- [46] J. Wu, Q. Zhang, and G. Xu, “Tiny imagenet challenge,” Tech. Rep.
- [47] F. Yu, A. Seff, Y. Zhang, S. Song, T. Funkhouser, and J. Xiao, “Lsun: Construction of a large-scale image dataset using deep learning with humans in the loop,” *arXiv preprint arXiv:1506.03365*, 2015.
- [48] M. Heusel, H. Ramsauer, T. Unterthiner, B. Nessler, and S. Hochreiter, “Gans trained by a two time-scale update rule converge to a local nash equilibrium,” *Advances in Neural Information Processing Systems*, vol. 30, pp. 6626–6637, 2017.
- [49] M. Bińkowski, D. J. Sutherland, M. Arbel, and A. Gretton, “Demystifying mmd gans,” *arXiv preprint arXiv:1801.01401*, 2018.
- [50] T. Salimans, I. Goodfellow, W. Zaremba, V. Cheung, A. Radford, and X. Chen, “Improved techniques for training gans,” *Advances in Neural Information Processing Systems*, vol. 29, pp. 2234–2242, 2016.
- [51] Z. Zhao, Z. Zhang, T. Chen, S. Singh, and H. Zhang, “Image augmentations for gan training,” *arXiv preprint arXiv:2006.02595*, 2020.
- [52] S. Zhao, Z. Liu, J. Lin, J.-Y. Zhu, and S. Han, “Differentiable augmentation for data-efficient gan training,” *Advances in Neural Information Processing Systems*, vol. 33, 2020.
- [53] X. Mao, Q. Li, H. Xie, R. Y. Lau, Z. Wang, and S. Paul Smolley, “Least squares generative adversarial networks,” in *Proceedings of the IEEE International Conference on Computer Vision*, 2017, pp. 2794–2802.

APPENDIX

A. *Generated Image Samples*

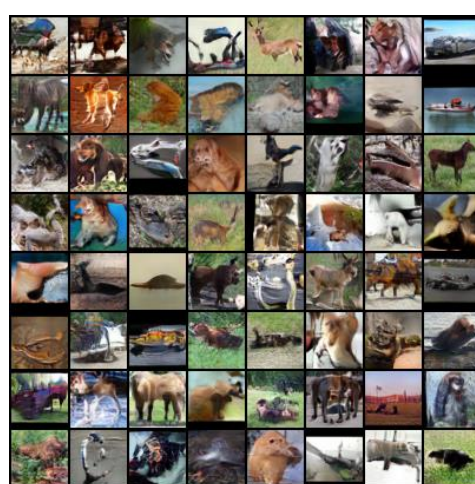
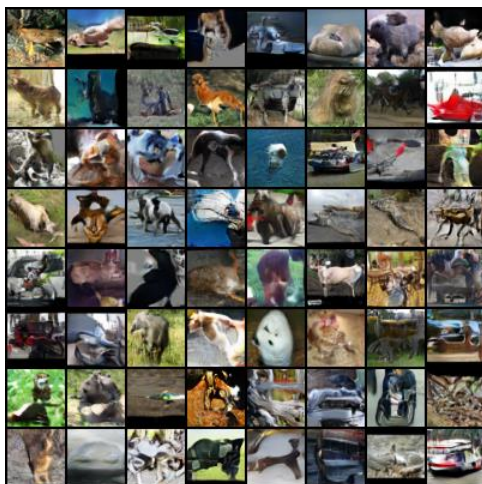
For qualitative comparisons, we present randomly sampled images generated by SSGAN and SSGAN-DAT for CIFAR-10, CIFAR-100, STL-10 and LSUN-Bedroom in Figures 9 and 10. We qualitatively observe that the images are more diverse and have higher quality after the use of DAT.



(a) CIFAR10

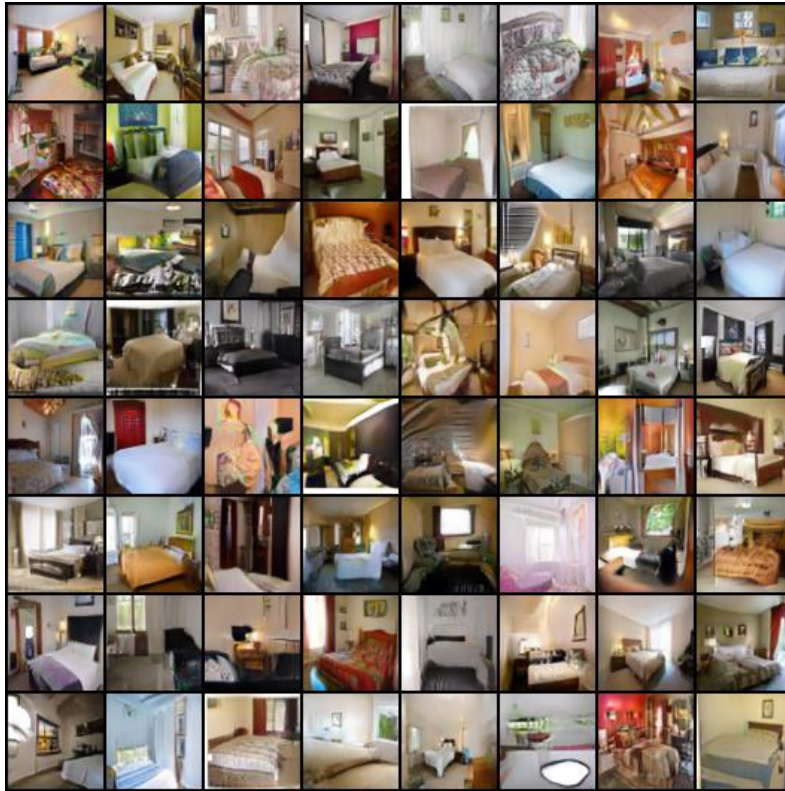


(b) CIFAR100

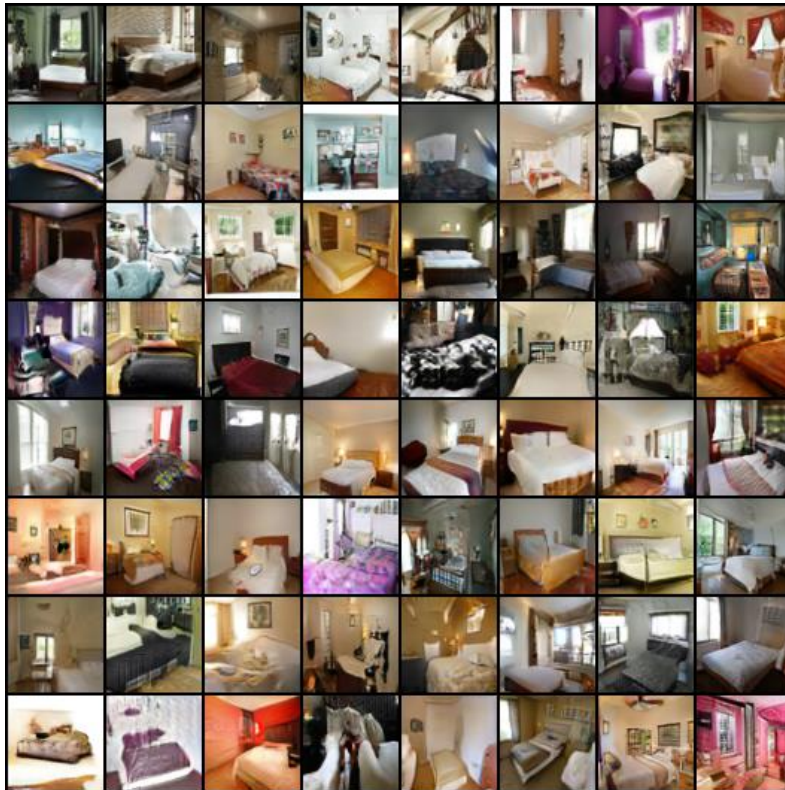


(c) STL10

Fig. 9: Randomly sampled and non-cherry picked images for SSGAN (left) and SSGAN-DAT (right) for CIFAR-10, CIFAR-100, and STL-10 datasets.



(a) SSGAN



(b) SSGAN-DAT

Fig. 10: Randomly sampled and non-cherry picked images for SSGAN (top) and SSGAN-DAT (bottom) for LSUN-Bedroom dataset.